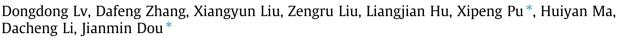
Separation and Purification Technology 158 (2016) 302-307

Contents lists available at ScienceDirect

Separation and Purification Technology

journal homepage: www.elsevier.com/locate/seppur

Magnetic NiFe₂O₄/BiOBr composites: One-pot combustion synthesis and enhanced visible-light photocatalytic properties



School of Materials Science and Engineering, Shandong Provincial Key Laboratory of Chemical Energy Storage and Novel Cell Technology, Liaocheng University, Liaocheng, Shandong 252000, PR China

ARTICLE INFO

Article history: Received 28 October 2015 Received in revised form 19 December 2015 Accepted 21 December 2015 Available online 22 December 2015

Keywords: NiFe₂O₄/BiOBr Photocatalyst Magnetic Combustion

ABSTRACT

Magnetic NiFe₂O₄/BiOBr composites with enhanced photocatalytic activity for degradation of Rhodamine B were synthesized by a simple one-pot combustion method. The structures, morphologies, optical, magnetic and visible-light photocatalytic properties of as-prepared samples were characterized. Experimental results showed that NiFe₂O₄/BiOBr composites with different molar ratios of NiFe₂O₄ to BiOBr (0–0.2) were successfully obtained. The photodegradation performance of as-prepared photocatalysts gradually increases with increasing molar ratio of NiFe₂O₄/BiOBr. The composite with a NiFe₂O₄/ BiOBr mole ratio of 0.2 shows the best visible-light photodegradation performance of Rhodamine B, which can be ascribed to the efficient separation of photo-generated electrons and holes. The magnetic properties of NiFe₂O₄/BiOBr photocatalysts ensure the magnetic separation by using a magnet. Moreover, no obvious deterioration was observed after six-cycle photodegradation experiments.

© 2015 Elsevier B.V. All rights reserved.

1. Introduction

Photocatalysis has attracted much attention due to its potential application in decomposing organic compounds for environmental remediation and solving the energy crisis [1–4]. Several photocatalytic semiconductor materials, such as TiO₂ and ZnO, have been widely used, but they have two shortcomings, that is, low efficiency under visible-light irradiation and difficulty in collecting after used [5-8]. Thus, the development of highly efficient visible-light-driven photocatalysts has become an appealing challenge [9,10]. In recent years, bismuth oxybromide (BiOBr) as a non-TiO₂ semi-conductor has received much attention due to its visible-light photocatalytic activities [11–14]. Various BiOBr micro/nano-structures, including nanoparticles, nanotubes, nanobelts, nanoplates, and microsheets, have been successfully fabricated by means of the hydrothermal [15], solvothermal [16], and microemulsion methods [17]. However, the band gap (Eg) of BiOBr is 2.91 eV, which makes it sensitive to a narrow region of visible light and endows it high recombination rates of electron hole pairs [18]. There are many strategies to improve photoactivity of photocatalysts, such as noble metal decoration [19], ion doping [1], and coupling of two or more semiconductor catalysts [20,21]. One of the effective ways to improve its photocatalytic ability is to combine BiOBr with other semiconductor materials to enhance its charge separation efficiency. For instance, Kong successfully prepared AgBr–BiOBr heterojunction photocatalysts with exceptional photocatalytic activity in visible-light degradation of Rhodamine B (RhB) [22]. An and coworkers reported the preparation of BiOBr/BiPO₄ heterostructure which exhibit much higher visiblelight photocatalytic activities than the individual BiPO₄ and BiOBr for degradation of model dyes MB [23].

NiFe₂O₄ with typical ferromagnetic properties, low conductivity and stable thermal ability is suitable for a wide range of applications in many fields including gas sensors [24], microwave devices [25], data storage devices [26]. Nickel ferrite (NiFe₂O₄), with an inverse spinel structure, exhibits ferrimagnetism deriving from a magnetic moment of antiparallel spins between Fe³⁺ ions at tetrahedral sites and Ni²⁺ ions at octahedral sites. NiFe₂O₄ has a E_g of 1.7 eV and broad absorption in visible region which are beneficial to photocatalysis. This expectation led us to prepare magnetic NiFe₂O₄/BiOBr composites with enhanced visible-light photocatalytic properties. Compared with above-mentioned reports about BiOBr based composite photocatalysts, NiFe₂O₄/BiOBr can be conveniently collected and separated after used.

In this work, we synthesized a series of $NiFe_2O_4/BiOBr$ composites (NFBB) with different molar ratios of $NiFe_2O_4$ to BiOBr by a simple one-pot combustion method. To our best knowledge, there





^{*} Corresponding authors. *E-mail addresses*: xipengpu@hotmail.com (X. Pu), dougroup@163.com (J. Dou).

is no report on the synthesis of NFBB photocatalysts. The results showed that the as-synthesized NFBB composites exhibited superior photocatalytic activity than that of pure NiFe₂O₄ and BiOBr. Furthermore, the plausible mechanism for the enhanced photocatalytic ability in the NiFe₂O₄/BiOBr heterostructures was proposed. Moreover, as-synthesized NFBB catalysts can be separated from solution after used in the presence of an external magnetic field, and their photostability were studied.

2. Experimental

2.1. Synthesis of NFBB composites

All reagents of analytical grade were obtained from Sinopharm Chemical Reagent Co. (Shanghai, China) and used without further purification.

The NFBB products with varying NiFe₂O₄ content were synthesized by a one-pot combustion method. First, 0.01 mol bismuth nitrate pentahydrate (Bi(NO₃)₃·5H₂O), was dissolved in 20 mL deionized water, followed by the addition of 2 mL concentrated nitric acid (65%) under vigorous stirring to obtain a transparent solution. Then appropriate amounts of iron nitrate nonahydrate $(Fe(NO_3)_3 \cdot 9H_2O)$ and nickel nitrate hexahydrate $(Ni(NO_3)_2 \cdot 6H_2O)$ were added to above Bi(NO₃)₃ absolution. Meanwhile, 0.03 mol ammonium bromide (NH4Br) and appropriate amount of citric acid were dissolved in 20 mL deionized water, and the obtained solution was quickly added into the above nitrates solution. Then the beaker was transferred to an electric jacket at a temperature of 300 °C in air, and the solvent was removed gradually. Finally, combustion reaction took place due to the exothermic redox reaction between nitrates and fuel, and the farinose samples were obtained. Samples with different molar ratios of NiFe₂O₄ to BiOBr (0, 0.05, 0.1, 0.2, 0.3) were synthesized and labeled as NFBB-molar ratio of NiFe₂O₄ to BiOBr. The molar mass of citric acid is equal to that of all nitrates. For comparison, the preparation of pure NiFe₂O₄ is according to the method from previous work [27].

2.2. Characterization

X-ray diffraction (XRD) patterns were recorded on a diffractometer (D8 Advanced, Bruker Co., Germany) with Cu Karadiation operated at 40 kV and 30 mA. The data were recorded in a 2θ range of 10–80° with a step width of 0.02°. Scanning (SEM) and transmission electron microscopy (TEM) were performed with a Gemini microscope (Zeiss Ltd., Germany) equipped with an energy-dispersive X-ray spectrometer (EDX) and a JEM-2100 microscope (JEOL Ltd., Japan), respectively. The Brunauer-E mmett-Teller (BET) specific surface areas of the samples were investigated by a Quantachrome Autosorb IQ-C nitrogen adsorption apparatus. The magnetic measurement was conducted with a vibrating sample magnetometer (Quantum Design Co., USA). Ultraviolet-visible (UV-vis) diffuse reflectance spectra (DRS) of samples and the absorption spectra of RhB solution were recorded on a UV-3600 spectrophotometer (Shimadzu, Japan). The photoluminescence (PL) spectra of the as-prepared samples were measured by an F-7000 spectrometer (Hitachi Ltd., Japan).

2.3. Photocatalytic test

Photocatalysis experiments were carried out in a home-made photocatalytic reaction box. A 300 W Xenon lamp with a UV cutoff filter (JB450) was positioned about 10 cm over a cylindrical container with a circulating water jacket for cooling. RhB was selected as a model pollutant to evaluate the photocatalytic activities of the as-prepared samples. Solid catalyst (0.1 g) was dispersed in 100 mL aqueous solution of RhB (10 mg/L). The solution was stirred in dark for 30 min to obtain a good dispersion and establish adsorptiondesorption equilibrium between the organic molecules and the catalyst surface. Decrease in the concentration of RhB solution was analyzed by recording the absorption band maximum (554 nm) in the absorption spectra and taken as the initial concentration (C_0). During the photocatalysis, 5 mL of the suspension was extracted at an interval of 20 min, and the absorption was measured after 3 min of centrifugation. The normalized temporal concentration changes (C/C_0) of RhB were obtained. In order to characterize the stability of NFBB photocatalyst, 6-cycle photodegradation for RhB was carried out. Each cycle lasted for 120 min. After each cycle, catalysts were washed by deionized water and absolute alcohol several times after magnetic separation for 3 min, and then re-dispersed in fresh RhB solution for the next cvcle.

3. Results and discussion

3.1. Characterization of NFBB composites

The XRD patterns of NiFe₂O₄, BiOBr and NFBB composites are shown in Fig. 1. Two sets of diffraction peaks can be observed from the patterns of samples, which can be indexed to the tetragonal BiOBr (JCPDS No. 09-0393) and the cubic spinel NiFe₂O₄ (JCPDS No. 10-0325). As shown in Fig. 1b, with the increasing molar ratio of NiFe₂O₄ to BiOBr, obvious diffraction peaks of NiFe₂O₄ are observed. Consequently, NFBB composites were successfully synthesized by the one-pot combustion method. However, a new weak peak for impurity indicated by asterisk is observed when the molar ratio is 0.3, and the peak is too weak to determined its phase.

The morphologies of neat BiOBr and the NFBB-0.2 were characterized by SEM, as shown in Fig. 2. A large number of uniform particles aggregated together to form micro-cluster structure in the pure BiOBr sample (Fig. 2a). However, NFBB-0.2 shows a flakelike morphology with nanoparticles attached on surface of flakes (Fig. 2b), and these nanoflakes are larger than the nanoparticles of pure BiOBr sample, as shown in the enlarged SEM images (Inset of Fig. 2a and b). The larger size of flakes of NFBB-0.2 endows NFBB-0.2 a smaller BET specific area (28.944 m²/g), however the BET specific area of pure BiOBr is $30.429 \text{ m}^2/\text{g}$. Furthermore, the NFBB-0.2 sample was characterized by EDX analysis, as shown in Fig. 2c. The elements Fe, Ni, Bi, Br and O are present in NFBB-0.2, and the atomic ratio agrees well with the stoichiometric composition of the sample. BiOBr and NFBB-0.2 were further characterized by TEM, as shown in Fig. 3. Obviously, as shown in Fig. 3a and b, two samples both exhibits sheet-like morphologies. However, the surface of NFBB-0.2 nanoplate is attached by nanoparticles, which is same with the SEM results. In the HRTEM image of BiOBr (Fig. 3b), the lattice fringes of 0.252 nm coincide with the fringe spacing of the (110) lattice plane of the tetragonal BiOBr. By comparison, in the case of NFBB-0.2 (Fig. 3d), besides the lattice fringes of 0.252 nm ((110) plane of tetragonal BiOBr), new fringes with spacings of 0.275 nm and 0.299 nm are observed and can be indexed to the (311) and (220) crystal planes of the cubic spinel NiFe₂O₄, respectively. According to the XRD, SEM, and TEM results, the nanoparticles attached on the nanoflake of NFBB should be spinel NiFe2O4.

The magnetic hysteresis loops of samples at room temperature are given in Fig. 4. Obviously, all samples show ferromagnetic behaviors. The saturation magnetization (Ms) of pure NiFe₂O₄ sample is 50.8 emu g⁻¹. In contrast, NFBBs have smaller Ms values, due to the presence of non-magnetic BiOBr. Moreover, Ms of NFBBs increases with increasing NiFe₂O₄ content. The ferromagnetic

Download English Version:

https://daneshyari.com/en/article/640223

Download Persian Version:

https://daneshyari.com/article/640223

Daneshyari.com